Conference Paper, Published Version

Rifai, Ismail; Le Bouteiller, Caroline; Recking, Alain

Numerical Study of Braiding Channels Formation

Numerical Study of Braiding Channels Formation

Ismail Rifai[1,2], Caroline Le Bouteiller[1], Alain Recking[1]
[1] IRSTEA centre Grenoble, France
[2] Ecole Nationale du Génie de l'Eau et de l'Environnement de Strasbourg, France
ismail.rifai@irstea.fr

Abstract— **In this study, we investigated the ability of a physics based 2-D model (TELEMAC2D coupled with SISYPHE) to reproduce the braiding dynamics from the initiation, starting from an initially flat bed with a central incision, to the evolution of the pattern resulting from different flow, sediment forcings and sediment transport formulas. The idealized river model remained close, in terms of dimension, to flume experiments. The choice of boundary conditions, taken as simple as possible, allowed to directly link the result to the constitutive relations used and an isolated analysis of the model capability to reproduce the morphology and the dynamic characteristic of braided streams. The simulation results showed that the model successfully reproduced the initiating phase of the braiding pattern.**

I. INTRODUCTION

Braided rivers are self-induced forms of alluvial streams which are characterized by a multichannel network separated by ephemeral exposed bars (see Fig. 1). Prevailing sediment inflow, high stream power and erodible banks are necessary conditions for braiding. Among the existing channel types of alluvial rivers, the braiding streams are - the less stable and the more active in terms of sediment transport, or more specifically, bedload transport [1].

Figure 1. Waimakarini River, New Zeland (Google Earth)

The reasons which lead to the initiation of the braiding of a stream are partially known. However, there is no scientific consensus yet. As cited in [2], one can consider two main reasons for both the initiation and the development of braiding: an abundant bed load and an easily erodible banks. The overloads encourage the first sediment deposition so it initiate the formation of the first central bar which will cause the deflection of the flow [3] and therefore the erosion of the banks and the widening of the mean stream bed. Furthermore, turbulence and the regime tendency to lower its Froude number can also be considered as factors for, respectively, initiating and developing the braiding pattern [4].

Braided rivers are particular in terms of their morphodynamics. Formed with a large gravel bed in which multiple channels cross and split; their global aspect is similar to braids. Their crossing channels are separated with gravel bars, which are very dynamic. Although, the channels can be slightly sinuous, they generally follow the orientation of the valley. One other aspect of braided rivers, the pattern or the bed form might seem chaotic and complex. Nevertheless, most of the time, the water flows only on half of the channels [5]. Also, the solid transport activity is limited to a narrow strip in the main channels [6].

In this work, we assessed the capabilities of the TELEMAC-MASCARET modeling system (TMS) to reproduce the dynamic of the braiding system from the initiation of the braiding pattern and the response of the numerical model to different types of settings. Prior to the numerical modeling work, a physical model was developed in the hydraulics laboratory of IRSTEA Grenoble in order to establish basis knowledge relative to braiding streams. Accordingly, some of the model's settings and calibration parameter were inspired from the flume experiments. Further details can be found in [7].

In the following, we will first present the numerical model configurations, secondly the simulations results and then conclusions regarding the TMS ability to reproduce the braiding streams dynamics will be drawn and discussed.

II. NUMERICAL EXPERIMENT

A. *Construction of the model*

The domain considered for the numerical simulations was 10,75m long and 1,15m wide, similar to the dimensions of flume experiments. A small rectangle was added upstream at the inlet in order to withdrawn the input. This proved to effectively eliminate some of the instabilities at the very first nodes. Therefore, the domain was described with an unstructured grid of triangular elements with 61212 nodes and a typical edge length of 1,5cm.

TELEMAC was run in depth averaged mode (2-D) and was fully coupled with SISPHE.

B. *Initial conditions*

The initial state from which the simulation starts is a flat sloping bed (3%) with a central incision of 10cm and a constant water depth of 2mm on the whole domain. This last condition didn't affect the behaviour of the model and was

chosen only in order to ensure the stability of the first time steps.

C. Boundary conditions

Before presenting the boundary conditions, it was suitable to first present how the following modelling work is organized (see Fig. 2).

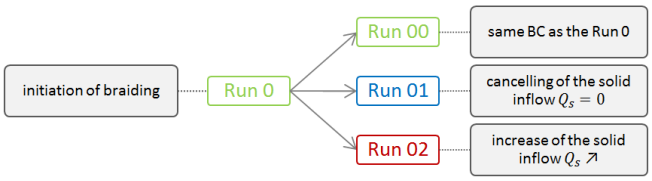

Figure 2. Organization of the runs

First, Run0 starts from the flat initial model presented before, Run0 was therefore the braiding formation model. Second, and once the braiding was established, three major runs followed. Run00 is the continuity of Run0. The boundary conditions were kept the same as prior Run0. The two other runs, Run01 and Run02 are, respectively, erosion and aggradation. In the first one, the sediment inflow was stopped, and in the second one, the sediment inflow was increased. The Table 1 presents the boundary conditions configuration for each run.

TABLE I. BOUNDARY CONDITIONS FOR EACH RUN

Runs	Inlet		Outlet	
	$Q_s(m^3/s)$	$Q_l(m^3/s)$	$Q_s(m^3/s)$	$Z_{free\ surface}(m)$
Run 0	7.46×10^{-7}	3.75×10^{-4}	Calculated with sediment transport formula	Constant (2 mm above the bed level)
Run 00				
Run 01	0			
Run 02	1.15×10^{-6}			

D. Modeling parameters

The 2-D simulations were performed using the finite element method for the hydrodynamics and the finite volume method for the morphodynamics. The scheme used for the advection of velocities and water depths were, respectively, the method of characteristics scheme and the mass-conservative distributive PSI scheme. The solver used for the hydrodynamic propagation step was the conjugate gradient on normal equation method and conjugate gradient method for the turbulence model.

Considering all these numerical parameters, and in agreement with the specified boundary conditions, the optimum time step of each iteration was therefore t=0,01s.

The turbulence model considered was the constant viscosity model, the advantage of this model is that it required a lower refinement level of the mesh compared to the K-epsilon and therefore reduces the CPU time. The overall viscosity coefficient (molecular + turbulent) was 10^{-6} m^2/s (water at 25 °C). This velocity diffusivity parameter had an impact on both the shape and extent of recirculation.

Regarding the bottom friction law, it is one of the most important hydrodynamics parameters which influence the water velocity and also the bed shear stress, which controls the sediment transport rate. It was taken the same in the whole computation domain. The used friction law was the Stickler's law with the a Strickler coefficient of K=50 $m^{1/3}/s$.

Moreover, the simulation parameters for the morphodynamic module were as follows.

The sediment used had a mean diameter of D_{50}=0,8mm. The use of uniform particle size allowed to conduct an analysis without consideration of the hiding and exposure effects. Furthermore, the sediment transport formulas used for the four runs (0, 00, 01 and 02) was the classical Meyer-Peter-Müller formula. In addition, Ashmore [8] and Van Rijn [9] formulas were used in other following runs.

The critical Shields number was taken equal to θ_c = 0,047 when Meyer-Peter-Müller formula or Van Rijn [9] formula were used. However, when the simulation was run with Ashmore [8] formula the critical Shields parameter was set to θ_c = 0,045.

In this work, we included the effect of the (transverse) slope on sediment transport. It allow to take in consideration the direct effect of gravity on particle on a sloping bed. Indeed, the gravity adds a force which can encourage or discourage the initiation of the transport, in other terms: the slope effect has an influence on the threshold shear-stress [10]. The critical Shields θ_c parameter was therefore adjusted via the Soulsby formula. Depending on the slope angle, the angle of repose and the relative direction of the flow to the slope direction, the threshold shear-stress value would either increase or decrease. The new critical Shields $\theta_{\beta c}$ parameter was calculated according to Soulsby formula.

On the other hand, the change of the direction of solid transport was also take in account by the use of deviation's formula from [11]:

$$\tan\alpha = \tan\delta - T\frac{\partial Z_f}{\partial n} \quad (1)$$

$$T = \frac{1}{\beta_2\sqrt{\theta}} \quad (2)$$

Where α is the direction of solid transport, δ is the direction of the bottom stress in relation to flow direction, Zf is the bed level, n the coordinate along the axis perpendicular to the flow and β2 an empirical coefficient taken equal to 0,85.

SISYPHE allows to take into account the influence of the secondary currents, such as helical or spiral flow effect, on sediment transport. Indeed, the bedload transported sediments are deviated from the main stream because of such effects. The sensitivity analysis conducted by [12] on his numerical model of braiding rivers highlighted the importance of the consideration of these effects. The deviation angle δ caused secondary currents effect was implemented in the model via Engelund formula:

$$\tan\delta = 7\frac{h}{r} \quad (3)$$

The coefficient α was taken equal to 1, in agreement with the recommendation to relatively smooth beds.

III. RESULTS

First, the Run 0 and Run 00 results are exposed in the same section. The second section presents the results of the Run 01 and the third the results of Run 02. Also, additional simulation models are presented.

A. Establishment of the braiding pattern (Run0 and Run00)

First, as the simulations started, one could notice the changes on the central incision. Indeed, the banks were eroded and therefore the central incision's width increased. The sediments coming from the inlet boundary added to the mobilized volume from the bank erosion contributed to the increase of the bed level. This, added to widening of the channel, increased the width-to-depth ratio. In other terms, the channel became shallow and therefore the sediment transport capacity decreased. The sediment were deposed and the first bars appeared.

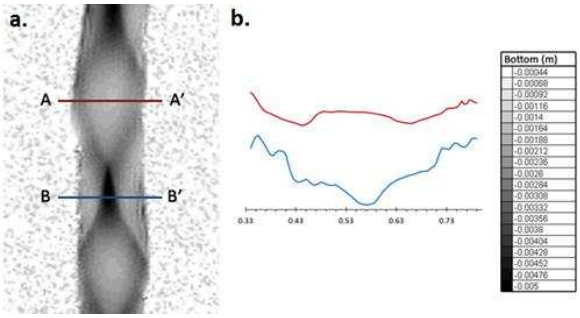

Figure 3. The formation of bars. a. the bed's topography Run 0, b. cross section of the bed, in red the cross section of a bar and in blue the cross section of a scour hole.

The bar developed a curved convex shape with a central "peak" (see Fig. 3) .This caused the water flow to split and flow on the sides of the central bar. Passing the central bar, the junction of the two channel streams (confluence) lead the increase of the transport capacity and the appearance of a pool. One could also notice the forward migration of this bars in the downstream direction.

This pool formation and migration processes are well described in literature [13]. The confluence of channels created a highly turbulent zone which destabilize locally the bed and lead to the digging of a scour hole. The migration of the channels and therefore their junction caused then also the migration of this scour hole.

This first phase lasted about 40 minutes. At a certain point, the bars were exposed and the continuous aggradation caused the elevation of the bed level. Consequently, some channels started flooding and the water start flowing on what could be assimilated to a flood plain. Therefore, if the shear stress was high enough, the incision of a new channel initiated (see Fig. 4). These observations suggested that the braiding initiates by combined aggradation and erosion processes. The forward migration of these bars toward the downstream direction was also observable on the model (Fig. 4).

After 1 hour, the bed morphology became similar to the braiding patterns observed in both in the field and flume experiments. The braiding morphology was rather realistic and the model shows several noteworthy morphologies typical to braiding rivers. After the first hour, to the end of Run0, the braiding developed but in a much slower motion compared to ti initiation.

Passing the second hour to the end of Run 00, the bed seemed to evolve and change. However, analyzing water depth, water velocities and solid discharge revealed that even if the bed relief seemed undulating and varying, the water mostly flowed in single channel. Consequently, one can state that the highly rippled bed forms are only the remainings of a previously braiding stream.

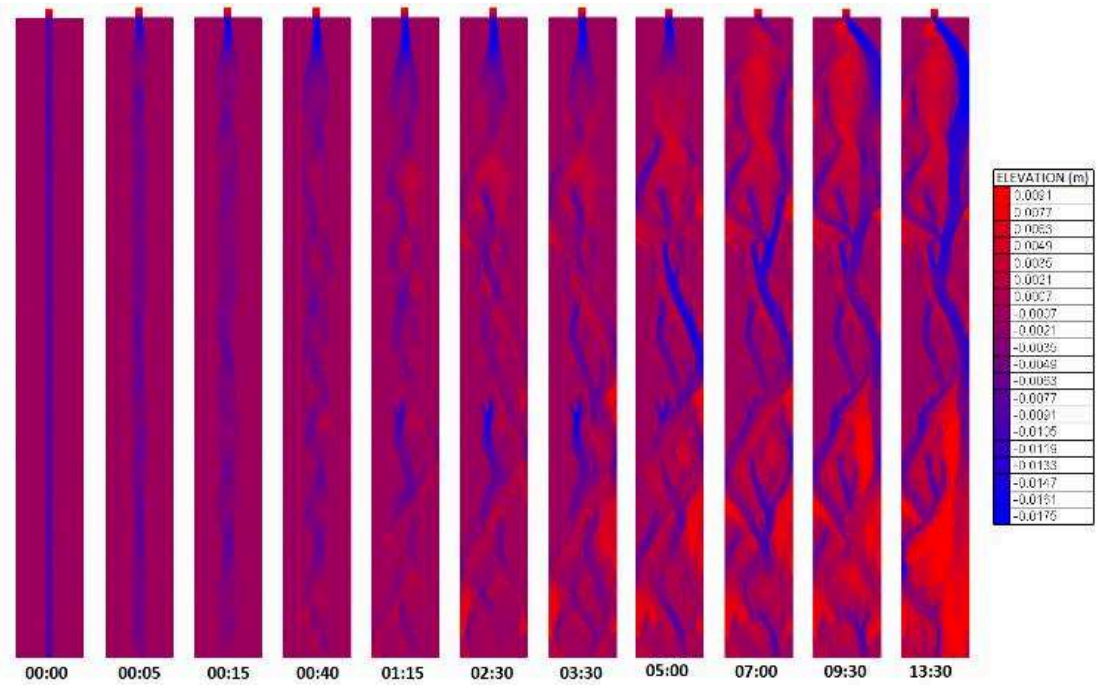

Figure 4. Run0-00: evolution of the bed through time.

The Bed Relief Index (BRI) reflects the transversal variability of the bed around the average elevation and the active-BRI is the BRI if we only take into account active channels elevations (here the threshold value over which a channel was considered as active was a water depths of h=2mm). Both are expressed in meters.

Fig. 5 shows the evolution of the BRI and active-BRI over time. The active-BRI was lower than the standard BRI because, at the beginning, not all the flow is contained in the first incision, and therefore a thin layer (lower than 2 mm) of water poured over the banks. During the first 30 min both the indices decrease, which is due to the shallowing of the central incision. This first profile smoothing phase was followed by a renewal of the transversal irregularities of the bed which indicated bar formation.

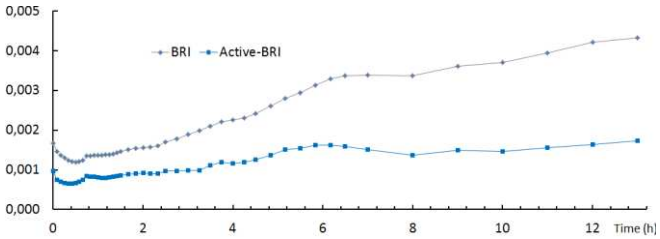

Figure 5. Evolution of the BRI and active-BRI of Run0-00

The bars emergence was also captured by the active-BRI. Indeed, a small decrease could be noticed around the first hour, whilst the standard BRI increased. The bed continued changing its transversal profile while a dry zone had emerged.

The continuous increase of the BRI reflected the bed's remodelling. However, passing the sixth hour, the BRI's evolution slowed and the active-BRI became almost constant. This ascertainment reflects a tendency of the system to convert to a single-thread channel: the water flow migration to a single channel phase was shown by the decay of the active-BRI and a slight increase of the standard BRI. Then, the single channel started incising, which increased the total horizontal variation of the bed but left the active active-BRI almost constant. The growing gap between the BRI and active-BRI proved that even though the bed is remodeled, only a small fraction conveyed the water.

In addition, we calculated three average slopes: the slope of the upstream half of the domain, the slope of the downstream half and the mean slope.

First thing noticeable, is that Run0-00 was characterized by three phases. The general shape of the bed started by becoming convex, then, after the 35 minutes, became concave, and once again became convex. The first phase was due to the deposition of inlet sediments at the upstream part of the flume as a response of the sudden widening of the domain. Consequently, the sediment deficit caused the erosion of the middle of flume, which sediment would be deposited in the downstream part. In addition, the profile shape seemed to translate in the downstream direction, the aggraded pile shifting would gradually reverse the convexity (passing from convex to concave), and again, when the sediment wave reached the downstream part, the bed regains its convex like shape. This process was clearly seen in the Fig. 6. Indeed, the conveying of the sediment wave affected the partial mean slopes.

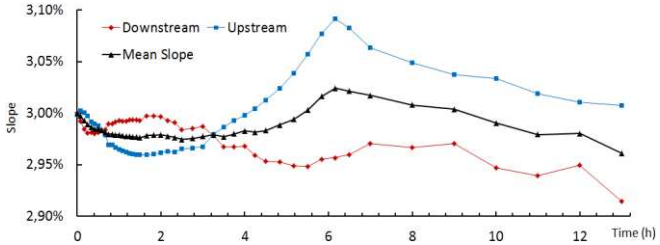

Figure 6. Evolution of the slope of Run 0-00.

However, slope decreasing indicated an adjustment of the topography in order to adapt to the boundary condition (or the control variable). This could indicate that the system was at sediment supply limitation. Nevertheless, at a certain point a width averaged slope accounting for the total width became somewhat irrelevant. In fact, the BRI and visual analysis of the bed topography showed that after the sixth hour the stream transform to a single-thread channel. Consequently, only the topography of a small fraction of the width would reflect the hydro-morphodynamical status of the system. Calculating the slope along the main channel showed agreement with this statement, for the slope of the main channel at the end of Run 00 was 2.59 %, which was less than the mean slope of the whole data extraction zone.

B. Erosion (run01)

In this part, we investigate the response of a braided model (resulting from Run0) to the cancelling of sediment feeding. The flow rate was kept constant and the sediment inlet was stopped.

The simulation results showed that the BRI increased as the bed evolves in time (see Fig. 7). The incision of a main channel added to previous bed variation, and therefore the BRI continued on increasing. However, the active-BRI only accounted of the variations of bed surfaces under water (the threshold value is taken equal to 2mm 2 mm)). In fact, one could notice the relatively slow evolution of the active-BRI,, which was a reflect of two phenomena: the narrowing of the main channel with the decrease of its width-to-depth ratio and the progressive conversion to a single-thread channel, then its ongoing narrowing, which happened from the upstream to the downstream.

In comparison to the values of Run0-00, which were also increasing, we could notice that the Run 01's values of BRI and active-BRI were higher, which revealed that the single channel resulting from Run01 was narrower.

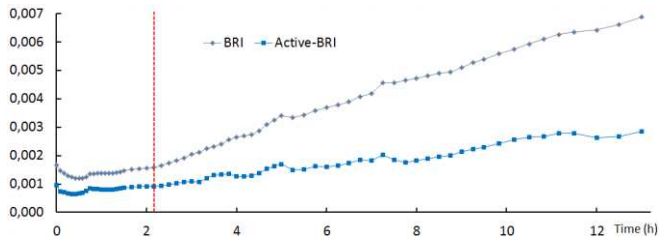

Figure 7. Evolution of the BRI and active-BRI (Run 01 starts at 02:15).

The mean slope of the whole bed continuously reduced along the simulation (see Fig. 8). This result agreed with general field and flume observations and also with the Lane's Balance principle. However, the upstream and downstream mean slope considered apart, showed how the slope adjustment process occurred. Indeed, the upstream slope remained lower than the downstream one for about 9 hours. The width average bed profile had a concave shape during this phase. These observations were the result of the transfer of the sediment budget from upstream to downstream, which described the slope adjustment process. After this adjustment period, the bed slope seemed to stabilize.

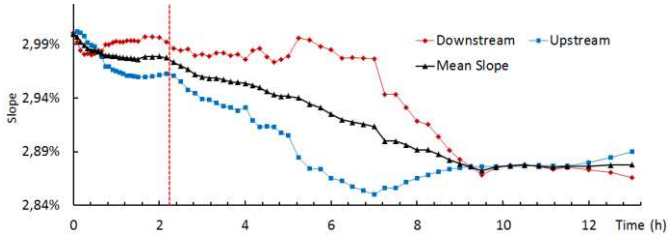

Figure 8. Evolution of the slope (Run01 starts at 02:15).

Considering the transformation of alluvial style to a single channel one. The slope of a width averaged profile became quite irrelevant. In that sense, the slope of the main channel was measured. The channel slope was equal to 1,99% which was less than the mean slope of the whole bed.

C. Aggradation (Run02)

In here, we investigate the response to braiding model (resulting from Run0) to the increase of the sediment feeding. The flow rate was kept constant and the sediment feeding was increased by 54%.

The BRI continued increasing, as in the two previous runs. However, the increase of the sediment feeding didn't maintain the braiding morphology.

The active-BRI showed that a certain equilibrium was reached after the 7th hour. The active-BRI remained almost constant, meaning that the dominant channel didn't incise nor flatten. However, the increase of the standard BRI combined with a constancy of the active-BRI indicated that the total bed's topography encountered some changes, but the average channel's shape remained at rest. In other terms, although it moved within the domain, the dominant channel's shape remained almost constant.

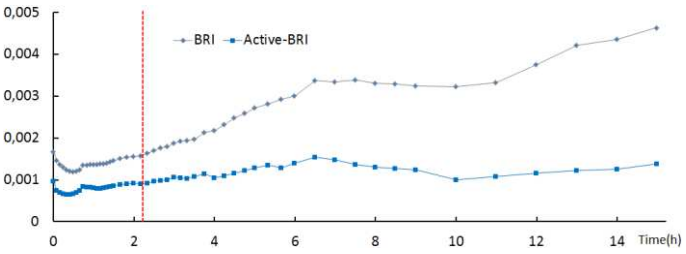

Figure 9. Evolution of the BRI and active-BRI (Run 02 starts at 02:15).

The slopes variations (see Fig. 10) remained of the ones of Run0-00. The profile's convexity changes compared well. A closer look to this slope variation showed that the shifting from the concave profile to a convex one happened sooner in this run than in Run0-00. The aggradation process at the upstream

part was accelerated by the abundant sediment feeding. The peak of the total and upstream slope at 06:30 was characteristic of the collapse of the sediment deposit at the inlet and its gradual propagation through the domain.

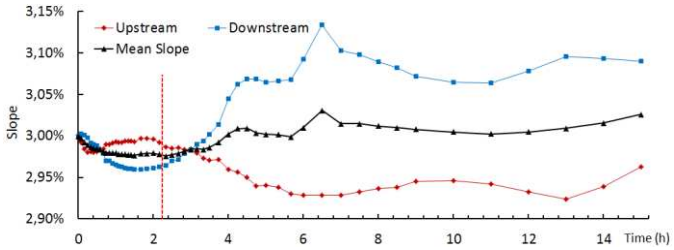

Figure 10. Evolution of the slope (Run02 starts at 02:15).

D. Additionnal results

The following is a short presentation of other braiding streams simulations. Their aim was to broaden the view of TELEMAC2D/SISYPHE abilities on reproducing braiding morphologies with the account of other parameters. Besides, the analysis of these new results would provide additional bases necessary to the assessment of the models strength and weaknesses. Hereafter, the models' results will be discussed briefly and mostly in a qualitative way.

1) Variation of the water inflow

Two additional model runs were simulated in order to investigate the influence of the variation of the water discharge on the maintaining of the braiding pattern. The first one accounted for the flow rate variation using a hydrograph with a randomly oscillating discharge over time. In the second one, the direction of the flow at the inlet was changed over time in a random motion.

On the one hand, the variation of the flow rate wasn't very conclusive. The hydrograph random variation didn't prevent the progressive transformation of the pattern to a single-thread channel. On the other hand, the random variation of the velocity vectors direction gave rather interesting results. The braiding pattern seemed more developed (see Fig. 11) and maintained longer than in the case of constant inflow direction.

2) Ashmore and Van Rijn

The Van Rijn [9] formula was already available in SISYPHE's subroutines and the Ashmore formula [8] was implemented in the model.

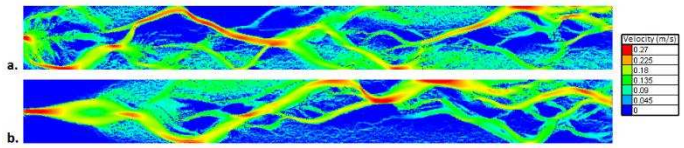

Figure 11. Water velocity field of the after 3 hours, a. with random variation of the inflow velocity vectors, b. with a constant direction of the inlet's water velocity vectors

The results produced by each one of these formulas were quite different (see Fig. 12). The beds topography seemed more evolved for the Van Rijn model. Compared to the results of the previous runs, one could state that the Ashmore formula [8] underestimated the sediment transport comparing to Meyer-Peter-Müller and Van Rijn [9] formulas.

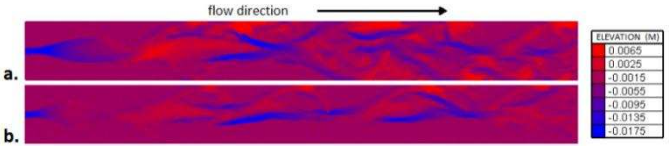

Figure 12. Elevation of the bed resulting after 3 hours with a. Van Rijn [9] transport formula and b. Ashmore's [8].

IV. DISCUSSION AND CONCLUSIONS

First, Run0-00 showed how the model initiated the braiding pattern. Indeed, at the beginning of the simulation, the bed started evolving as a reaction of the hydrodynamics and sediment inflow. The results showed realistic initiation processes in agreement with flume observation as described by [8], [13], [14]. Observations of the bed evolution after 15 minutes showed the co-occurrence of the two modes and also, to some extent, the superposition of theses said modes. This was also observed in flume experiments [7], and therefore gave a good appreciation of the model's accuracy in capturing such processes.

However, the observations on the bed's evolution, BRI, active-BRI, slopes and volumes changes agreed with the typical initiation's path of braiding streams. However, passing a certain time, the model failed maintaining the braiding pattern and the flow gradually merged into a single channel. This behaviour could be related to insufficient sediment feeding, or to inadequate representation of the processes controlling bars and bank's erosion. The following runs, Run01 and Run 02, investigated the effect of, respectively, the cancelling of the sediment inflow and its intensification. On the one hand side, the model respond as expected to the cancelling of solid feeding. A single channel, with a lower slope, and conveying all the flow rate, formed progressively from upstream to downstream. On the other hand, Run 02 didn't respond as expected. Indeed, the increase of sediment discharge didn't prevent the transformation of the active pattern into a single-thread channel.

At the end, after 13 hours, the three simulations converged to a single channel stream, each of which had a different width, sinuosity and slope. As one could foresee, the higher the sediment inflow, the steeper the main channel's slope.

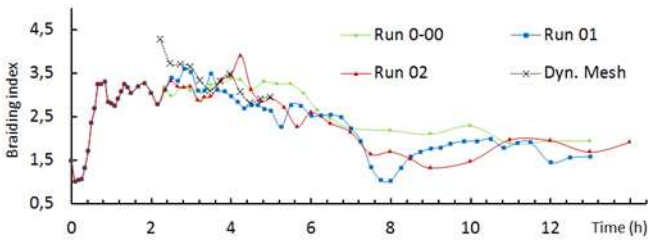

Figure 13. Comparison of the braiding indices [14] of the runs.

Besides, the comparison of the braiding indices [14] in Fig. 13 confirmed that the models failed in sustaining the braided pattern for the three runs. The decrease of the braiding index

was almost the same, and happened at the same time, regardless of the boundary conditions. This suggests that, besides the boundary conditions, other causes were involved in the systems' tendency to converge to a single channel configuration:

- The lack of variation of the inflow discharge;
- The unvarying inlet location;
- The insufficient refinement of the mesh as it doesn't represent well both the hydrodynamics and erosion processes near the banks.

The second part of the modelling work related to the influence of additional model's parameters. First, the random variation of the velocities direction at the inlet nodes proved to be moderately effective in terms of sustaining the braiding pattern. This fact underlined the importance of a sustained perturbation of the flow to maintain a braiding pattern. However, as the simulation forwarded in time, the braiding was abandoned in favour of a main single channel. Also, when the flow direction was varied the braids only maintained longer, but did not evolve into another analogous braiding pattern. Which weighted in favour of the lack of representativeness of banks erosion processes as a limiting factor for braids development.

Second, the changing of the transport formula influenced the formation of braids, which developed sooner when Van Rijn [9] bedload formula was used. For a same shear stress value, different load formulas gave different results. However, one should keep in mind the effects of the nonlinearity of sediment transport equations as stated by [15]. The presented Ashmore formula [8] has been developed with the account of the active width averaged shear stress, Meyer-Peter-Müller and Van Rijn on the basis of narrow flume experiments, whilst TELEMAC2D computes the shear stress per node. Consequently, the causes of these differences of results can be partially justified by the nonlinearity of the load equations.

Indeed, in [15] Recking showed that such effects are even greater when the exponent of the shear stress is high. The exponents of the sear stress in Ashmore [8], Meyer-Peter-Müller and Van Rijn [9] formulas were respectively 1.37, 1.4 and 2.1. This results highlighted the importance of care on the choice of transport formulas depending on the dimension of the problem, for the transition from a 1D to a 2D model wouldn't be without consequences.

The discussion above showed how the model succeeded on representing the braiding initiation and, in opposition, it failed on maintaining this braiding pattern. In fact, the lack of channels dynamics was apparent and is to be attributed the models failure on sustaining dynamic and mobile braids. But, before starting the discussion of the numerical effects on the braiding evolution, it would be suitable to first recall that during the modelling work, the setting of the boundary conditions for instance, proved to be delicate task and rather limitative. In addition, in many circumstances an unrealistic and massive accumulation of sediment happened at the boundary nodes, or, exaggerated erosion/aggradation occurred in located nodes. These model instabilities compelled additional effort in the model calibration.

In that sense, the models lack of dynamic couldn't be addressed by lowering the implication coefficient for it would deteriorate the model stability. Conversely, increasing the numerical diffusion would produce smoothed results and therefore damp, to a certain extent, the morphodynamics.

Besides, the model stability was also conditioned by the mesh quality, which in turn impacts, not only, the CPU time, but also the results' precision. Furthermore, in a 2-D simulation the edge length would force the minimal channel width. In fact, channels narrower than twice the distance between two nodes would not form. The small channels (in terms of number of nodes per cross section) evolutions is very constrained. In addition, a very high slope in a coarse 2-D mesh will cause the relative elevation of two consecutive nodes to be high, which will yield to bad interpretation of the free surface transversal profile.

Which brings the discussion to the last point: the impact of mesh refinement on the representatively of the banks and therefore the impact on the bars' erosion processes. Yet, one could first recall the observations made on the models' gradual transition to a single-thread channel in Run 00 and Run01. The bed initially braided progressively formed a relatively wide, deep and low slope channel which carries the imposed flow rate. This conversion reminds of the observation of [16] resulting of the effects of vegetation on braiding channels in flume experiments.

Indeed, the experiments results showed that the vegetation caused the previously bare braiding pattern to transform to a meandering like stream. This transformation of the morphology is caused by the development of the plants and the ensuing effects, such as, the slowing the rate of channels' widening and definition floodplains. In this sense, the constraint of the mesh's level of refinement as a limiting factor for small channel incision and evolution can be compared to the effects of vegetation on discouraging the reactivation channels, which is typical to braiding streams dynamics [5]. This lack of braiding's dynamics was also observed in other numerical modelling studies [12].

Therefore, the two major limitations of the 2-D model can be related to the refinement of the mesh. However, as stated before, the number of nodes had a direct incidence on CPU efforts. Consequently, reducing the nodes spacing can make the simulation too much time consuming or even impossible. Besides, the constant refinement of the mesh could reveal to be inefficient for it would also increase the mesh definition in low interest areas. Conversely, the adaptation of the mesh to the bed's relief (close nodes in sloping areas like banks and bars' edges for instance) can reveal to be only efficient in short time scale studies since the channels pattern changes over time. The solution is therefore to have a mesh which will constantly adapt for example to the beds topography.

Fig. 14 shows an example of an adaptive mesh. In fact, the resulting grid is refined near the banks and left coarse in relatively flat zones. Indeed, multiplying the nodes defining a bank would increase the model accuracy in these high interest regions and therefore allow better erosion processes representation.

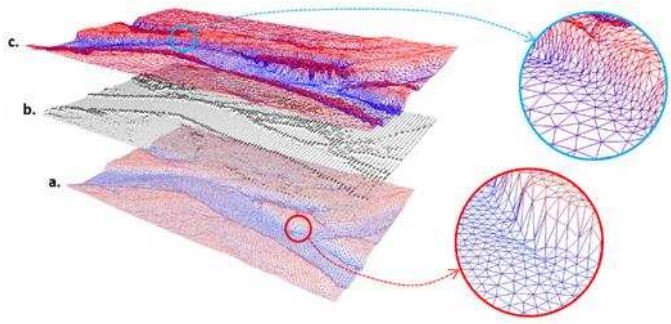

Figure 14. Example of mesh adaptation process. a. the initial mesh with constant nodes' spacing, b. the detection of high bed's variation areas, c. adapted mesh to the bed's relief with a high resolution in sloping zones.

This last solution was tested. Indeed, an additional model was built furthering in time the last state of Run0 with the same boundary conditions. In this run, the mesh was updated every 15 minutes. The density of the unstructured was set depending of the bathymetry gradient: tightened in steep areas and widened in flat ones. The results, however, were not very conclusive. The braiding pattern evolved to a single thread channel, which translated by a decrease of the braiding index (see Dyn.Mesh in Fig. 14). Nevertheless, the BRI and active-BRI were significantly remained lower than for the Run00. This could be partially related to the smoothing of the bed's topography generated by the frequent updating of the mesh. In addition, after 3 hours, the resulting bed was different from the one of Run00. This emphasises the effect of the mesh on both the hydrodynamics and morphodynamics and therefore the prediction of the braidplain evolution.

Other aspect of the mesh refinement process that should be considered with care is the choice of the threshold criterion. In the example above, the mesh refinement was linked to the variation of the topography along the cross section. This method will have the disadvantage of unnecessarily increasing the resolution even for dry undulating lands for example. Many criterions could be chosen, for instance:

- 2-D variation of the bed's elevation;
- Water depths variation;
- Velocity gradient;
- A weighted combination of these parameters.

Finally, the present report aimed at modelling the sediment dynamics in a braiding streams. To do so, a 2-D coupled hydro-sedimentary model (TELEMAC2D coupled with SISYPHE) was used. The braiding stream model was inspired from prior flume experiments. Three major cases were simulated in order to investigate the braiding formation and evolution in response to different forcing. Additional runs were done so as to broaden the assessment of the model capabilities.

The main conclusions of this report relate to the model's ability to generate realistic braiding pattern and representing its dynamics. In that sense, the simulation results showed that the 2-D model succeeded in replicating the braiding initiation phase and the resulting pattern was presented realistic features. However, the braiding pattern didn't maintain in any of the simulations. Besides, the additional runs showed that the model reacted accurately to other forcings such as variation of the initial slope, widening of the braidplain, but failed on simulating sediments grading effect in the case of bimodal material. It also revealed that inlet perturbations improve the maintaining of braids, however, it didn't address the issue completely.

Though, one can state that most of the model's strengths mentioned above are not only specific to TELEMAC, but can also be associated to other 2-D physics based model. In fact, the success of TELEMAC on reproducing the braiding formations for example, is mostly associated to the fact that the mathematical formulations of the physical phenomena are accurate and thorough. Still, TELEMAC-MASCARET modelling system, with its high flexibility and extensibility, allows benefiting from the advantages of a physical based model.

However, the main disadvantages (which can also be exported to other 2/3-D models) were, on the one hand, the high computation time. The time required for a simulation is linked to the model's time scale, the space scale, the numerical scheme and its level of refinement. Indeed, compared to other models, such as branches, neural or cellular, the general 2/3-D general models were the most time consuming. On the other hand, the uncertainties of the results are even more significant in the case of complex pattern as the braiding rivers. A single simulation with one set of boundary conditions doesn't give enough information to speculate on a braiding river's future evolution. This last issue could be addressed by a Monte Carlo approach. Although it would multiply the computation time, it remains a promising path for future development, especially with the continual increase of computational power and the parallelization of codes.

In addition to this last TELEMAC-MASCARET modeling system development outlook, one could also add the development of a vegetation module which will account of the effect of vegetation growth on the hydro-morphodynamics. And also, the consideration of adaptive finite volume methods with a dynamic mesh with an adaptation criterion based on physical assumptions and/or error posteriori estimates.

ACKNOWLEDGEMENT

We acknowledge the contribution and review of Erik Mosselman during the Braiding Rivers Workshop 2014.

Special thanks to Pablo Tassi for the advice and the recommendations.

REFERENCES

[1] S. A. Schumm, "Patterns of Alluvial Rivers," Annu. Rev. Earth Planet. Sci., vol. 13, no. 1, pp. 5–27, May 1985.

[2] J.-R. Malavoi and J.-P. Bravard, Eléments d'hydromorphologie fluviale. 2010, p. 224.

[3] L. Leopold and M. Wolman, River channel patterns: braided, meandering, and straight. 1957, p. 85.

[4] M. S. Yalin, River mechanics. Pergamon Press, 1992, p. 219.

[5] P. Ashmore, "Intensity and characteristic length of braided channel patternsThis paper is one of a selection of papers in this Special Issue in honour of Professor M. Selim Yalin (1925–2007).," Can. J. Civ. Eng., vol. 36, no. 10, pp. 1656–1666, Oct. 2009.

[6] P. Ashmore, W. Bertoldi, and J. Tobias Gardner, “Active width of gravel-bed braided rivers,” Earth Surf. Process. Landforms, vol. 36, no. 11, pp. 1510–1521, Sep. 2011.

[7] I. Rifai, A. Recking, and C. Le Bouteiller, “Two Dimensional Modeling of Sediment Dynamics in Braiding Rivers,” 2014.

[8] P. Ashmore, “Bed load transport in braided gravel-bed stream models,” Earth Surf. Process. Landforms, vol. 13, pp. 677–695, 1988.

[9] L. C. Van Rijn, “Sediment transport, part i: bed load transport,” J. Hydraul. Eng., vol. 110, no. 10, pp. 1431–1456, 1984.

[10] R. Soulsby, Dynamics of Marine Sands: A Manual for Practical Applications. London: Thomas Telford Publications, 1997, p. 256.

[11] A. M. Talmon, N. Struiksma, and M. C. L. M. Van Mierlo, “Laboratory measurements of the direction of sediment transport on transverse alluvial-bed slopes,” J. Hydraul. Res., vol. 33, no. 4, pp. 495–517, Jul. 1995.

[12] F. Schuurman, W. a. Marra, and M. G. Kleinhans, “Physics-based modeling of large braided sand-bed rivers: Bar pattern formation, dynamics, and sensitivity,” J. Geophys. Res. Earth Surf., vol. 118, no. November, Dec. 2013.

[13] P. Leduc, “Étude expérimentale de la dynamique sédimentaire des rivières en tresses,” Université de Grenolble, 2013.

[14] P. E. Ashmore, “How do gravel-bed rivers braid?,” Can. J. Earth Sci., vol. 28, no. 3, pp. 326–341, Mar. 1991.

[15] A. Recking, “An analysis of nonlinearity effects on bed load transport prediction,” J. Geophys. Res. Earth Surf., vol. 118, no. 3, pp. 1264–1281, Sep. 2013.

[16] M. Tal and C. Paola, “Effects of vegetation on channel morphodynamics: results and insights from laboratory experiments,” Earth Surf. Process. Landforms, vol. 35, no. 9, pp. 1014–1028, Feb. 2010.